

Bayesian Inference of Infectious Disease Transmission from Whole-Genome Sequence Data

Xavier Didelot,^{*1} Jennifer Gardy,^{2,3} and Caroline Colijn⁴

¹Department of Infectious Disease Epidemiology, Imperial College London, London, United Kingdom

²Communicable Disease Prevention and Control Services, British Columbia Centre for Disease Control, Vancouver, BC, Canada

³School of Population and Public Health, University of British Columbia, Vancouver, BC, Canada

⁴Department of Mathematics, Imperial College London, United Kingdom

*Corresponding author: E-mail: xavier.didelot@gmail.com.

Associate editor: Eduardo Rocha

Abstract

Genomics is increasingly being used to investigate disease outbreaks, but an important question remains unanswered—how well do genomic data capture known transmission events, particularly for pathogens with long carriage periods or large within-host population sizes? Here we present a novel Bayesian approach to reconstruct densely sampled outbreaks from genomic data while considering within-host diversity. We infer a time-labeled phylogeny using Bayesian evolutionary analysis by sampling trees (BEAST), and then infer a transmission network via a Monte Carlo Markov chain. We find that under a realistic model of within-host evolution, reconstructions of simulated outbreaks contain substantial uncertainty even when genomic data reflect a high substitution rate. Reconstruction of a real-world tuberculosis outbreak displayed similar uncertainty, although the correct source case and several clusters of epidemiologically linked cases were identified. We conclude that genomics cannot wholly replace traditional epidemiology but that Bayesian reconstructions derived from sequence data may form a useful starting point for a genomic epidemiology investigation.

Introduction

Infectious disease outbreak investigation typically involves both field work—interviews that establish links between patients and/or exposures to a source of infection—and molecular epidemiology, in which laboratory typing of pathogen isolates is used to identify related cases. Data from both streams are considered together to reconstruct the outbreak, identifying its origins and pathways of onward transmission. Ideally, the reconstruction aids in the real-time management of the outbreak and guides public health policy and practice in preventing future occurrences.

Molecular epidemiology has recently undergone a revolution with the advent of next-generation genome sequencing. With the cost of sequencing a complete bacterial genome now comparable to that of a gold-standard typing analysis (Sabat et al. 2013), traditional molecular methods for investigating bacterial disease outbreaks are increasingly being replaced by genomics (Didelot, Bowden, et al. 2012; Köser et al. 2012; Didelot 2013; Le and Diep 2013). Techniques such as multilocus sequence typing interrogate approximately 0.1% of a bacterial genome. In contrast, whole-genome sequencing permits identification of sequence variation across the complete genome. Given the short timescales over which outbreaks typically occur, only a small number of single nucleotide changes are expected between outbreak isolates. This diversity is not captured by traditional typing methods but can be identified and leveraged for outbreak reconstruction using whole-genome approaches.

A first approach to exploit this emergence of genomic data is to define a threshold for the number of genomic differences

above which direct transmission is unlikely (Eyre et al. 2013; Walker et al. 2013; Walker et al. 2014). This has the advantage of being a simple way to rule out when transmission did not happen, but reconstructing transmission when it did happen is less straightforward. Most reconstructions published to date rely heavily upon fieldwork data, and the utility of genome sequencing for inferring transmission events in the absence of these data—which, for a given outbreak, may be incomplete or unavailable—remains unclear, particularly for diseases characterized by periods of latency or chronic infection, during which substantial within-host genetic diversity may arise. Although most investigations include a phylogenetic analysis of the outbreak isolates, phylogenetic trees do not directly correspond to transmission trees and cannot, as such, identify specific person-to-person transmission events (Pybus and Rambaut 2009). In a densely sampled outbreak, all cases will appear as tips of the phylogenetic tree, when in fact some of these cases will have transmitted to others, so internal branching events are also associated with sampled hosts.

Nevertheless, it should be possible to infer transmission from sequence data using alternative approaches, and several such methods have been proposed (Cottam, Thébaud, et al. 2008; Jombart et al. 2011; Lieberman et al. 2011; Morelli et al. 2012; Ypma et al. 2012; Jombart et al. 2014). These methods typically identify transmission events as branching events in a phylogeny, and they do not consider within-host genetic diversity. This simplification may be appropriate for pathogens with a fairly small generation time—the time that elapses between a host becoming infected and causing other infections—but not for those with long generation times,

© The Author 2014. Published by Oxford University Press on behalf of the Society for Molecular Biology and Evolution.

This is an Open Access article distributed under the terms of the Creative Commons Attribution License (<http://creativecommons.org/licenses/by/3.0/>), which permits unrestricted reuse, distribution, and reproduction in any medium, provided the original work is properly cited.

Open Access

latency, and carriage. In these organisms, one can expect several nucleotide changes to accrue within a single host, with different individual lineages being transmitted onward to secondary cases. Examples include *Clostridium difficile* (Didelot, Eyre, et al. 2012; Eyre et al. 2013), *Mycobacterium tuberculosis* (Gardy et al. 2011; Walker et al. 2013), *Staphylococcus aureus* (Young et al. 2012; Golubchik et al. 2013; Harris et al. 2013), and *Helicobacter pylori* (Kennemann et al. 2011; Didelot et al. 2013). Excluding the possibility that multiple distinct genetic lineages of a pathogen—distinguished by only a few mutations—can be present within a host can lead to serious misinterpretation of putative transmission events (Ypma et al. 2013).

Furthermore, current methods for transmission inference do not leverage the capabilities of time-calibrated phylogenetic inference methods. Given the importance of factors such as branch length in inferring the underlying host contact network structure from a phylogeny (Robinson et al. 2013), an inference method that incorporates sampling times and a molecular clock analysis is preferable to one using neighbor-joining, maximum parsimony, or other simplified tree-building algorithms.

With the increasing use of genomic epidemiology, a method capable of inferring transmission events from genomic data alone while also considering within-host diversity offers an important tool for outbreak reconstruction. Here, we present a Bayesian inference scheme based on timed phylogenetic trees that can be run independently of epidemiological data or weighted with whatever fieldwork data is available, such as timing and duration of infectivity, level of infectivity, and geographic location. Our method rests on a within-host pathogen population genetic model, under which different lineages may be transmitted to secondary cases. We first reconstruct a timed phylogenetic tree and then infer the underlying transmission network, given the observed phylogeny. This second step is achieved by coloring the branches of the phylogeny with a unique color for each host so that a change of color represents transmission between hosts (fig. 1). This two-step approach represents a formalization of a previous approach to reconstruct transmission events on top of a timed phylogeny (Cottam, Wadsworth, et al. 2008). We make use of existing robust methods for phylogenetic inference, such as Bayesian evolutionary analysis by sampling trees (BEAST) (Drummond and Rambaut 2007) and ClonalFrame (Didelot and Falush 2007), and employ a novel Bayesian methodology to infer a transmission network via a Monte Carlo Markov chain (MCMC). We apply our method to simulated data to illustrate its performance, and to a real-world data set to reconstruct the transmission of *M. tuberculosis* in a densely sampled outbreak.

Results

Within-Host Diversity Affects Placement of Transmission Events on a Phylogenetic Tree

To assess the impact of within-host diversity on the inference of transmission events from a phylogeny, we simulated a transmission tree—the set of specific person-to-person

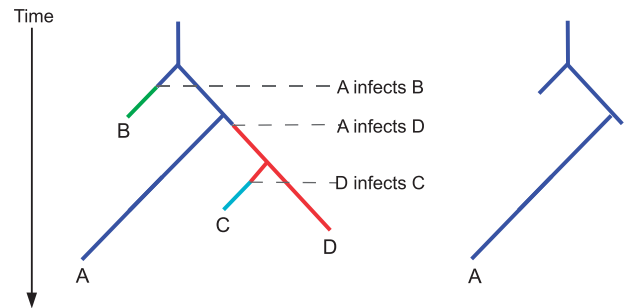


FIG. 1. The colored genealogical tree (left). Each host isolate corresponds to a unique color. A lineage is colored according to the host it was in at the corresponding time. When a lineage changes from color c_i to c_j (forward in time), this represents i infecting j . Each color may not persist in the tree after the time of the corresponding tip, because this is the recovery time of the host. The subtree restricted to a single color (right) is the part of the tree inside the corresponding host; lineages are taken from this tree at the recovery time and the times when the host infected others.

transmission events within an outbreak—and genealogies arising from this tree under two scenarios of effective population size. We modeled an outbreak in a susceptible population of size $N = 100$, with a per year recovery rate $\gamma = 2$ and per year, per contact infectivity rate $\beta = 0.02$. The expected number of infected individuals in a susceptible-infectious-removed (SIR) model is $R(\infty)$, such that $R(\infty) = -\frac{\gamma}{\beta} \log \frac{N-R(\infty)}{N-1}$ (Allen 2008), which here is $R(\infty) = 13.51$. A transmission tree T was simulated under these conditions, with ten individuals infected (fig. 2A).

If the effective population size within hosts is $N_e = 0$, then within-host diversity is zero, and transmission events coincide exactly with coalescent events of the phylogeny (fig. 2B). This assumption simplifies the relationship between the transmission tree T and the genealogy G and may be appropriate for infections with a short incubation time. However, in cases of latent disease, chronic infection, or long carriage periods, this assumption may not be valid. An example of this is asymptomatic carriage of *S. aureus*, which can persist within a host for months to years (Scanvic et al. 2001; Eveillard et al. 2004; Marschall and Mühlemann 2006) so that the recovery rate $\gamma = 2$ above is realistic, but the parameter $N_e g$, corresponding to the product of effective population size N_e and generation time g (i.e., duration of a replication cycle), is on the order of 100 days (Young et al. 2012; Golubchik et al. 2013).

Simulating a genealogy G under the same transmission tree T but with $N_e g = 100/365 = 0.274$ year illustrates the complex relationship between G and T that arises under a model of within-host diversity (fig. 2C), with transmission events no longer corresponding to coalescent events. In particular, it is now possible for the genomes from two hosts A and B to share a common ancestor more recently than with the genome from a third host C, even if C infected both A and B. An example of this in figure 2C is provided by host 1, who infected both hosts 2 and 3. In spite of this, 2 and 3's genomes are more closely related to each other than to 1's, because both 2 and 3 were infected by a lineage from 1 that is different

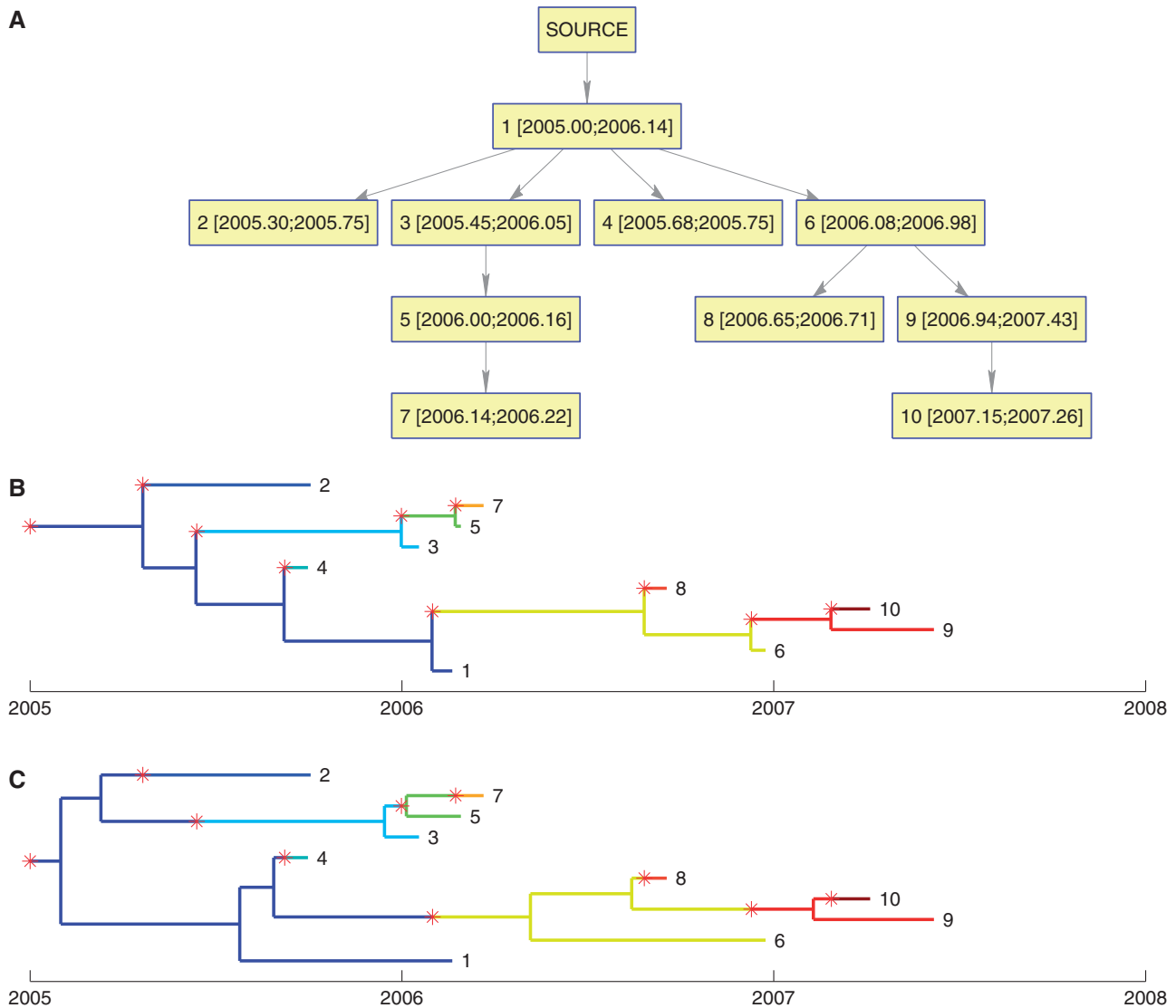


FIG. 2. (A) Transmission tree simulated with $N = 100$, $\gamma = 2$, and $\beta = 0.02$. The numbers in square brackets represent the time of infection and removal of each individual, respectively. (B) Genealogical tree simulated conditional on the transmission tree in (A) and with parameter $N_{eg} = 0$. Transmission events are indicated by red stars and a change in branch color. (C) Same as in (B) but with parameter $N_{eg} = 0.274$.

from the one that was sampled. If no within-host diversity was assumed, the genealogy in [figure 2C](#) precludes the possibility of 1 infecting both 2 and 3. Under our more realistic model with $N_{eg} = 0.274$, these transmissions become a possibility.

MCMC Inference of a Transmission Network from a Phylogeny Captures Known Transmission Parameters and Events

To determine whether the known events and parameters of transmission tree T could be inferred from a genealogy G , we applied our MCMC method to the simulated data set in [figure 2C](#). The MCMC was run for 100,000 iterations with the first half (burn-in) discarded. This took approximately 5 min on a desktop computer, and several independent runs were compared to ensure good convergence and mixing of the chain.

The inferred rate of infectivity β had posterior mean 0.021 (95% CI 0.010–0.038) capturing the correct value of $\beta = 0.02$, while the inferred rate of removal γ had posterior mean 1.82 (95% CI 0.88–3.17), also capturing the correct value of $\gamma = 2$. The inferred effective population size N_{eg} had posterior mean 0.49 (95% CI 0.02–2.49), which included the correct value of $N_{eg} = 0.274$, but that was also compatible with N_{eg} values up to an order of magnitude higher or lower than the correct value. This result reflects the difficulty of precisely inferring N_{eg} , especially as only ten individuals were infected. In a separate simulation with β equal to 0.05, such that $R(\infty) = 89$ hosts became infected, all parameters were more precisely reconstructed, with CIs for β , γ , and N_{eg} of 1.9–2.4, 0.04–0.06, and 0.19–2.11, respectively.

The posterior sample of transmission trees inferred based on the phylogeny in [figure 2C](#) was summarized using a graph representing all transmission events with posterior probability above 10% ([fig. 3A](#)). All ten correct transmission events are

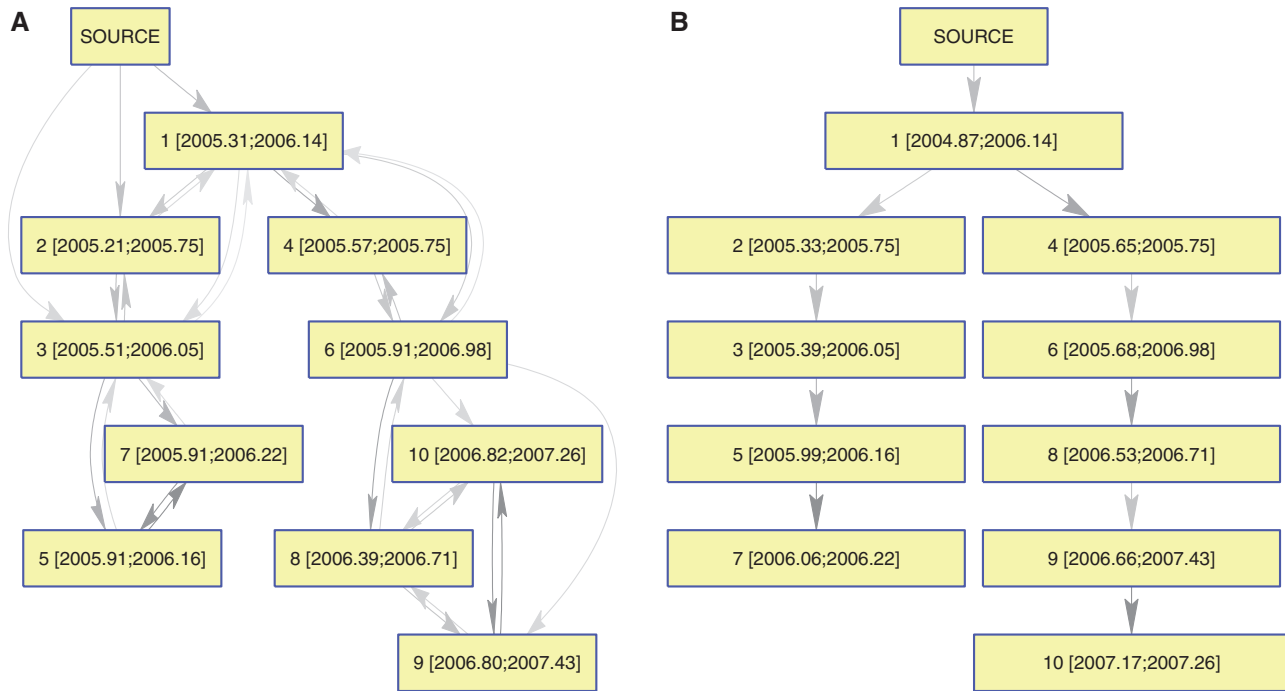


Fig. 3. (A) Network representation of the posterior distribution of transmission trees for the simulated data set shown in figure 2C. Nodes represent hosts, and the numbers within square brackets to mean inferred infection time and the known removal time. Edges represent a posterior probability of transmission of at least 10%, with a darker edge indicating a higher probability. (B) Point estimate of the transmission tree obtained by taking the optimal branching tree in the network shown in part (A).

present, but incorrect events are also contained in the graph, particularly the reverse of correct edges, making it difficult to distinguish infector from infected. With 30% of the posterior probability, host 1 was correctly identified the most likely source case (fig. 2A), but hosts 2 and 3 were also likely sources, with 25% and 17%, respectively. Overall, 33% of the posterior probability weight was carried by correct edges, with the remaining two-thirds of probability supporting transmission events that did not actually occur in the simulation. We used Edmonds' algorithm (Gibbons 1985) to find the optimal branching tree within the graph carrying the maximum posterior weight to identify the most likely transmission scenario. In the resulting point estimate of the transmission tree, seven of the ten simulated transmission events were recovered (fig. 3B).

One hundred scenarios analogous to the one shown in figure 2 were generated, each using the same parameters β , γ , and N_{eff} and each including ten infected individuals. Inference was performed for each of the hundred simulated data sets. On average, we found that correct transmission events carried 27% of the posterior probability weight. In each simulation, there are only ten correct transmission events, including transmission from an external source to the first case, out of a total of a hundred possible events (each of the ten hosts can infect any of the other nine, plus ten choices for transmission from the external source to the first case). Correct edges therefore carry, on average, almost four times more weight than incorrect edges: $(0.27/10)/(0.73/100) = 3.7$.

Reconstruction of a *M. tuberculosis* Outbreak Data Set

To assess the performance of our inference method on a real-world data set, we applied it to an outbreak of tuberculosis for which a hypothesized source case had been identified and for which epidemiological data supporting several further transmission events was available. A BEAST phylogeny (fig. 4A, supplementary fig. S1, Supplementary Material online) indicated that most of the inferred transmission events occurred after the source case (K02) recovered, meaning the source could have infected eight other people at most—eight being the number of unique lineages present in the tree at the source's recovery time—and that the source harbored significant within-host diversity. The clock rate estimated by BEAST had a posterior mean of 1.15×10^{-7} (95%CI 0.39×10^{-7} to 2.00×10^{-7}), consistent with previous estimates in *M. tuberculosis* (Ford et al. 2011; Walker et al. 2013).

We used the MCMC approach to infer transmission networks under two scenarios: one based only on the phylogenetic tree (fig. 4C) and one in which posterior probability weights were modified using epidemiological data (fig. 4D), including infectivity, infectious period, and geographic location (supplementary fig. S2, Supplementary Material online, shows the posterior mode in both cases). Although both graphs placed the suspected source K02 as central to the network, the modified network displayed both a lower clustering coefficient (0.483 vs. 0.596) and a higher average per-edge posterior probability (0.302 vs. 0.253), meaning that the modified network contained fewer bidirectional events, displayed a more web-like layout suggestive of waves of

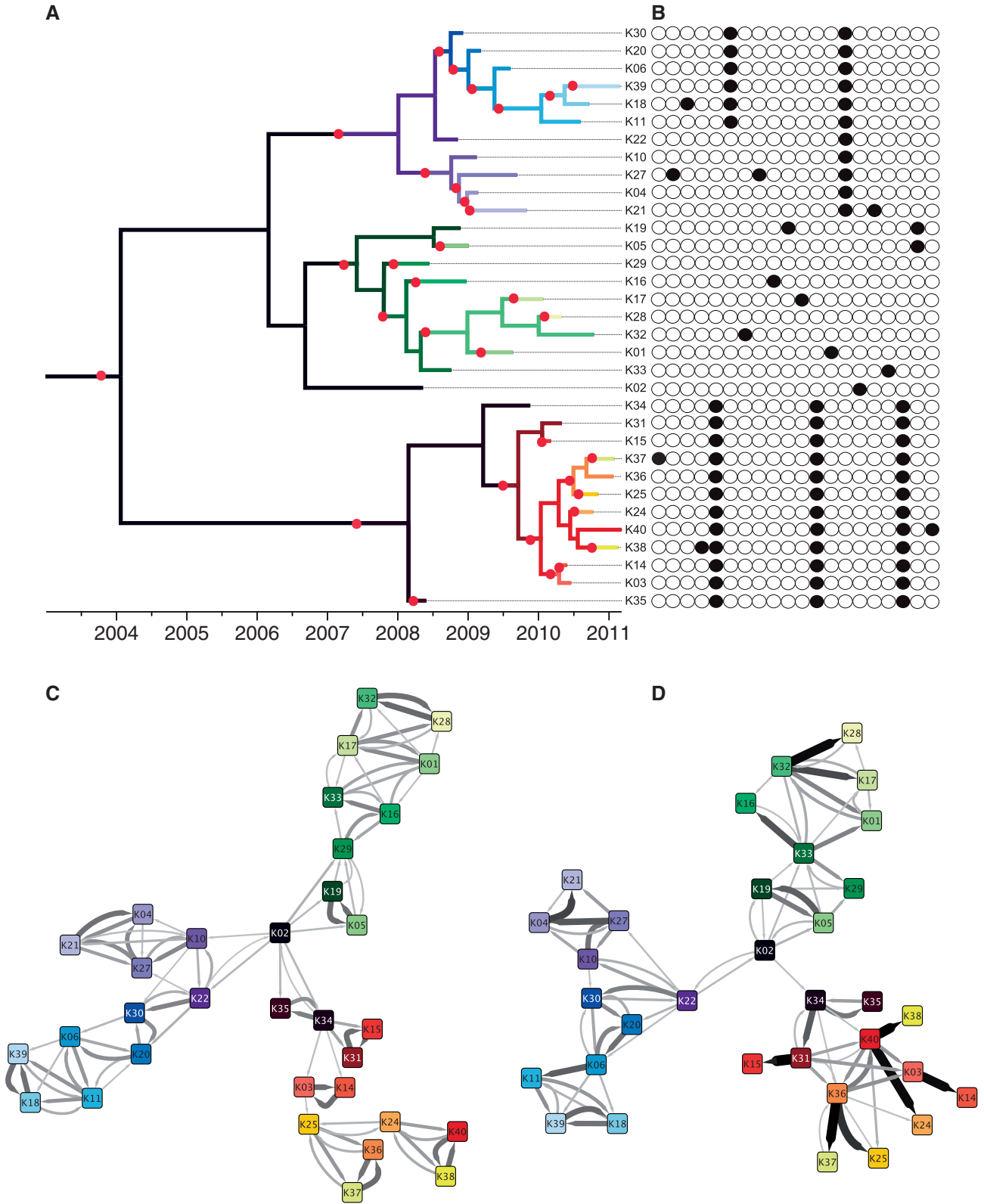


FIG. 4. Application to a real-world tuberculosis outbreak. (A) Phylogenetic tree inferred by BEAST. (B) SNVs differentiating the isolates. (C) Transmission network inferred without epidemiological modification. (D) Transmission network inferred with epidemiological modification. In (C) and (D), edges are shown with width and shading proportional to their posterior probability, except edges with low probability that are omitted. In (A), the phylogenetic tree is colored according to the consensus transmission tree from (D) and using the same unique colors for each host as in (C) and (D).

transmission rather than chains, and returned more high-probability events.

Comparing inferred transmission events to known epidemiology revealed that both the basic and modified networks did capture aspects of known epidemiology, but in different ways. Among eight contacts sharing a sleeping space with the source case, three were identified by both reconstructions, two were present only in the basic reconstruction, and one was present only in the modified reconstruction. Another reported household contact between two cases was not returned in the basic reconstruction but was present in the modified version. Both inferred networks recapitulated a cluster of three cases linked to a specific sleeping location; in the basic model, the cluster appears as a complete subgraph with roughly equal probabilities for all six edges, while in the modified version, it is clear that a single individual infected two other cases. We also examined the 15 transmission events with the highest probabilities in the modified reconstruction and found that three were well supported by epidemiological information, seven were possible given the known locations and contacts of cases, two did not appear to have an epidemiological linkage between the predicted infector/infected, and three were highly unlikely.

The three unlikely transmissions involved the three cases known to reside in a different geographic location than the other outbreak cases and thought to have been infected by a visiting traveller from the outbreak community. In the basic reconstruction, this scenario is mostly recapitulated—the traveller infects two further cases. In the modified version, despite including an adjustment for geographic location, the traveller does not infect any of the other three cases nor are they infected by individuals with a travel history to the other community.

The parameters estimated without and with epidemiological modification were similar, with $(N_{eg}, \beta, \gamma) = (1.48, 0.0037, 1.29)$ and $(1.21, 0.0032, 1.23)$ respectively. This value of the removal rate γ indicates that, on average, 15 months elapsed between infection of a host and its detection. We interpret the transmission rate β in terms of the basic reproduction number $R_0 = \beta N / \gamma$, the expected number of secondary infections caused by a case in a susceptible population. Because $N = 400$, we calculate $R_0 = 1.15$ (95%CI 0.73–1.9) in the basic reconstruction and $R_0 = 1.03$ (95%CI 0.65–1.69) in the modified reconstruction. This relatively low number is expected for tuberculosis in a low-burden, highly resourced setting like the one studied here (Dye and Williams 2000).

For simplicity, the networks described above were based on a single phylogeny, namely, the maximum credibility tree returned by BEAST. However, there was significant uncertainty in the BEAST posterior, as illustrated by a DensiTree plot (Bouckaert 2010) (supplementary fig. S3, Supplementary Material online). We therefore inferred transmission trees separately for each of the 100 trees sampled by BEAST, and the aggregated results are shown in supplementary figures S4 and S5, Supplementary Material online, for the application without and with epidemiological modification, respectively. In the case of the latter, accounting for the uncertainty in the

phylogenetic tree does not result in a great increase in uncertainty for the reconstructed transmission tree.

Discussion

We present a Bayesian inference method for reconstructing transmission events in a densely sampled outbreak using time-labeled genomic data. By modeling within-host evolution as a neutral coalescent process, we are able to account for within-host genetic diversity and accurately ascribe infection events to a host harboring multiple lineages of a pathogen—an issue critical to the reconstruction of diseases with latent or asymptomatic carriage periods and/or chronic infection. We first reconstruct a phylogeny, leveraging the strengths of existing packages for phylogenetic inference such as BEAST (Drummond and Rambaut 2007), and next infer a transmission tree using an efficient MCMC procedure.

Recently, an approach was proposed to relate phylogenetic trees to transmission trees (Ypma et al. 2013), using a similar decomposition to ours; they simultaneously inferred a phylogeny and a transmission tree for a data set on 12 farms infected with foot-and-mouth disease (Morelli et al. 2012). Their focus was on sampling and joint inference given a specific within-host population model and a sharply defined incubation period. In contrast, our method is very rapid and can be applied to large (densely sampled) outbreaks, it is applicable to infections with long and variable infectious periods, it exploits the capabilities of BEAST, and infers rather than specifies the in-host effective population size. We are also able to flexibly incorporate additional field epidemiological data of various types.

Our results demonstrate that even if the genomic data was perfectly informative about the phylogeny, as in our simulations, considerable uncertainty is present in the transmission network when a realistic model of within-host evolution is taken into account. Although true events are captured, they are often eclipsed by other potential events and cannot be completely identified, even with methods that extract the subgraph with maximal posterior probability weights. This contrasts with previous approaches to outbreak reconstruction that equated phylogenetic branching with transmission and may be too assertive when within-host diversity exists. Our Bayesian approach captures this uncertainty. In practice, another source of uncertainty comes from the fact that the phylogeny is never known exactly but only informed to some extent by the presence of genetic variations between the sequenced genomes. This uncertainty in the phylogenetic inference is fully captured by BEAST, which returns a sample of trees from the posterior distribution given the genomic data. Accounting for this phylogenetic uncertainty into the inference of the transmission tree can then be achieved by applying our method to each tree in the BEAST posterior sample (Nylander et al. 2008; Parker et al. 2008).

When applied to a real-world data set, the method based only on genomic data correctly inferred the most likely source case and several key transmission clusters supported by field data. We found however that the inference was significantly improved when it was based on

both genomic and epidemiological field data, something that our Bayesian method is well suited to accommodate. Any epidemiological information, or indeed a different model, can indeed be integrated into the prior for the transmission tree without affecting the remainder of the method. This illustrates the important point that genome sequencing in a public health context does not make epidemiological data redundant, but instead should be seen as a complementary stream of information. Even in the future when sequencing will become so cheap that multiple genomes can be sequenced from all hosts, we believe that pure genomic epidemiology will not replace classical epidemiology. It is also important to note that, in a retrospective study, overall patterns of transmission are of more interest to public health than precise inference of who infected whom. Our method suggests that genomic information can shed light on whether outbreaks tend to occur as long chains of transmission or as large bursts from single hosts, and whether transmissions tend to be associated with specific environments or hosts, even if individual transmission events remain uncertain.

Like any model-based statistical analysis, our method makes a number of assumptions, some of which might not be appropriate for every application. The within-host evolutionary dynamic is modeled by a simple coalescent process with constant population size (Kingman 1982). This could easily be relaxed to allow for variation in the within-host population size following infection while staying in a coalescent framework (Griffiths and Tavaré 1994). However, our specification represents a natural choice because it is the simplest possible choice of model with only a single parameter $N_e g$. Very little is known about the within-host evolutionary dynamics of most infectious diseases, but the use of a more complex model could be justified, for example, if it led to a better marginal likelihood as measured by a Bayes factor (Kass and Raftery 1995). Our model also assumes that the transmission bottleneck is complete. This would be more difficult to relax as any other choice would imply that some genetic diversity rather than a single variant can be transmitted from infector to infected, and therefore that the common ancestor of two isolates from the same host might be in a different host. Again, very little is known about this property for most infectious diseases, but among the few microorganisms where this was formally investigated, data suggest the bottleneck is very strong if not complete, for example, in HIV (Edwards et al. 2006; Keele et al. 2008; Haaland et al. 2009; Boeras et al. 2011).

The main limitation of the method as presented here is that it assumes that all cases comprising an outbreak have been sampled. This assumption was acceptable for the tuberculosis application, given the surveillance and reporting systems in place in this setting, but clearly would not be appropriate in all applications—for example, diseases with milder symptoms where cases may go unrecognized. However, our two-step approach provides a good starting point to investigate these outbreaks too. The phylogeny inferred in the first step does not assume full sampling, and the coloring in the second step could be redefined so that a color corresponds not just to a single host but rather to a host plus

all intermediate cases up to the next sampled case. Or alternatively, the number of colors could be allowed to vary and be greater than the number of sampled individuals, which would require the use of a reversible-jump MCMC (Green 1995) to deal with the resulting transdimensional parameter space. Additional parameters, such as the proportion of unsampled infected hosts, would be required to modify the model in this way, but the general approach of coloring the phylogeny will remain valid.

Materials and Methods

Model for the Epidemiological Process between Hosts

For the epidemic between-host spreading process, we consider a stochastic, continuous time Markov chain (CTMC) version of the general SIR epidemic model (Allen 2008). In a population of known size N , the parameters of this process are the infection rate β and removal rate γ . If the state of the process at time t is (S_t, I_t, R_t) , denoting the number of susceptible, infected, and removed individuals, respectively, then transition to the state $(S_t - 1, I_t + 1, R_t)$ happens at rate $\beta S_t I_t$ and transition to the state $(S_t, I_t - 1, R_t + 1)$ happens at rate γI_t . The former event is a transmission and the latter a removal. The process is started in the state $(S_0 = N - 1, I_0 = 1, R_0 = 0)$ and is run until the epidemic finishes at $I_t = 0$.

This basic process has been extensively studied, especially in a Bayesian framework where inference can be performed using an MCMC (O'Neill and Roberts 1999; O'Neill 2002). Let n denote the number of individuals who have been infected, that is, the number of removed individuals at the end of the process. Let T denote the transmission tree, where each node is one of the n infected individuals and edges represent transmission events. In our notation, T contains the information of who infected whom and when, as well as when individuals were removed. Simulation of a transmission tree T given the parameters N , β , and γ can be done using the Gillespie algorithm (Gillespie 1976).

Model for the Genealogical Process within Hosts

We consider that when each individual is removed, a single genome from the infectious agent is isolated and genotyped. The genealogical relationships between these genomes can be represented as a timed genealogy G , where leaves correspond to the n genomes (one from each host) and internal nodes represent common ancestors of the genomes. The genealogy G not only depends on the transmission tree T but also depends on the within-host evolutionary dynamics (Alizon et al. 2011) and the transmission bottleneck (Bergstrom et al. 1999; Grenfell et al. 2004). For simplicity, we model within-host evolution as a neutral coalescent process (Kingman 1982) with constant population size N_e and average generation time g , which corresponds to the duration of a pathogen replication cycle. In this model, any two lineages within a host coalesce at constant rate $N_e g$, which is therefore the sole within-host parameter of interest. Furthermore, the transmission bottleneck is assumed to be complete so that only a single genomic variant is transmitted from infector

to infected. This transmitted genome is a random sample from the infector’s pathogen population at the time of transmission.

Under these assumptions, the genealogy G can be simulated given a transmission tree T and parameter $N_e g$ as follows. In a first step, n subtrees are generated corresponding to the genealogical process within each host, and in a second step, these subtrees are pasted together in order to produce G . For the first step, the within-host genealogy of each host i is simulated independently of each other. The genealogy within host i has a single root at the time when i was infected, a leaf at the time when i was removed, and a leaf for each host that i infected at the time when these transmission events happened. Each within-host genealogy is generated using the coalescent with temporally offset leaves (Drummond et al. 2002) with coalescence rate $N_e g$ and using rejection sampling on the coalescent tree (Tavare et al. 1997) to ensure that a single lineage exists at the time when i became infected. For the second step, the pasting is done for each transmission event. For example, if A infected B at time t in the transmission tree T , then the subtree of A contains a leaf at time t and the subtree of B has its root at time t , and pasting is done between this leaf and this root. Repeating this pasting for all transmission events completes the generation of the genealogy G .

Bayesian Decomposition

Our approach assumes that all n infected individuals are known and that their removal times are also known. Based on the genomes sampled from each of the n individuals, the timed genealogy G is reconstructed, and for the time being, we assume that G is known exactly. Because the times of the leaves of G represent the removal times of the n individuals, our notation G includes these removal times but not the times of infection. Due to the within-host genealogical process, transmission events do not occur at branching points in the genealogy. The aim of the inference is to infer the epidemiological parameters β and γ , the within-host evolutionary parameter $N_e g$ and the transmission tree T . The posterior distribution of interest is therefore

$$\mathbf{P}(\beta, \gamma, N_e g, T | G) \propto \mathbf{P}(G | N_e g, T) \mathbf{P}(T | \beta, \gamma) \mathbf{P}(\beta) \mathbf{P}(\gamma) \mathbf{P}(N_e g). \tag{1}$$

The last three terms represent the prior distribution of the parameters β , γ , and $N_e g$, which we take to be exponential(1), and it remains to specify $\mathbf{P}(G | N_e g, T)$ and $\mathbf{P}(T | \beta, \gamma)$.

First, the term $\mathbf{P}(G | N_e g, T)$ in equation (1) represents the probability of the observed genealogy given the transmission tree and within-host parameter $N_e g$. We relate a transmission tree T to the genealogy G by associating each point on G to a host. This can be visualized as a “coloring” of the branches in G : each host i is represented with a unique color c_i , and a branch segment is colored with c_i if it corresponds to evolution that happened within host i . Transmission events therefore correspond to point on G where the color changes and do not, in general, coincide with branching times in the genealogy. The same host may harbor several lineages ancestral

to our sample at the same time, which can be visualized on the tree. Figure 1 illustrates this visualization and our notation. For a given host i , we can consider the tree G_i obtained by looking only at the branches of G that are colored with c_i . This tree G_i corresponds to the evolutionary process within host i and has a number of leaves n_i equal to one plus the number of hosts infected by i .

To find $\mathbf{P}(G | N_e g, T)$, we exploit the fact that the subtrees G_i correspond to evolution within each host $i = 1..n$, and so are independent of each other. Because the distribution is conditional on T , the dates d_{ij} of the $j = 1..n_i$ leaves in G_i are known (corresponding to all transmissions from i plus the removal of i). The date r_i of the root of G_i is also known because it corresponds to the infection of host i . This leads to the decomposition:

$$\mathbf{P}(G | N_e g, T) = \prod_{i=1}^n \mathbf{P}(G_i | N_e g, d_{ij}, r_i). \tag{2}$$

The term $\mathbf{P}(G_i | N_e g, d_{ij}, r_i)$ is the probability under the coalescent model with rate $N_e g$ of the timed genealogy G_i given the dates of its leaves, d_{ij} , and conditional on having only one ancestor by the time r_i of the infection of host i . If this last condition was not present (i.e., if r_i was a very long time ago), then this distribution would be that of the coalescent with temporally offset leaves as described by Drummond et al. (2002). The additional condition corresponds to the fact that the most recent common ancestor (MRCA) of the leaves has to be more recent than the date of infection because the transmission bottleneck is absolute.

To calculate $\mathbf{P}(G_i | N_e g, d_{ij}, r_i)$, we consider the n_i leaves in increasing order of age. For each leaf j , we consider adding it on the genealogy formed by the previous leaves $1..j - 1$. The first (most recent) leaf corresponds to a linear genealogy with probability 1. The second leaf has to coalesce with the linear genealogy of the first leaf before the infection time r_i . The third leaf has to coalesce with the genealogy formed by the first two leaves before the infection time r_i , etc. This process is repeated for all leaves so that the genealogy formed at the end is the complete G_i . When adding leaf j , let A_j denote the sum of branch lengths in the genealogy formed so far between the time of leaf j and the time where it coalesces with an ancestor of a previously considered leaf. Similarly, let B_j denote the sum of branch lengths between the time of leaf j and the time r_i . A_j is exponentially distributed with parameter $N_e g$, but this distribution is truncated by $A_j < B_j$ to ensure that coalescence happens before time r_i . We therefore deduce that $\mathbf{P}(G_i | N_e g, d_{ij=1..n_i}, r_i)$ can be calculated as follows:

$$\mathbf{P}(G_i | N_e g, d_{ij=1..n_i}, r_i) = \prod_{j=2}^{n_i} \frac{\exp(-A_j / (N_e g))}{N_e g (1 - \exp(-B_j / (N_e g)))}. \tag{3}$$

This now completely specifies $\mathbf{P}(G | N_e g, T)$ from equation (1).

The term $\mathbf{P}(T | \beta, \gamma)$ in equation (1) represents the probability of the full epidemiological process given the epidemiological parameters. T includes the times of all infection and removal times. Let $t_{i=1..2n}$ represent the list of all these event

times (i.e., n infections plus n removals), sorted chronologically, and let $e_{i=1..2n}$ be equal to 0 for infections and 1 for removals. At any time t , the number of susceptible, infected, and removed individuals is given by

$$\begin{pmatrix} S_t \\ I_t \\ R_t \end{pmatrix} = \begin{pmatrix} N \\ 0 \\ 0 \end{pmatrix} + \sum_{\substack{i=1 \\ t_i < t}}^{2n} (1 - e_i) \begin{pmatrix} -1 \\ 1 \\ 0 \end{pmatrix} + e_i \begin{pmatrix} 0 \\ -1 \\ 1 \end{pmatrix}. \quad (4)$$

By considering the probability of each event in turn, we deduce that

$$\mathbf{P}(T | \beta, \gamma) = \prod_{i=2}^{2n} (\beta I_{t_i} S_{t_i} (1 - e_i) + \gamma I_{t_i} e_i) \exp(-(\beta S_{t_i} I_{t_i} + \gamma I_{t_i})(t_i - t_{i-1})) / I_{t_i}. \quad (5)$$

The denominator in equation (5) comes from the fact that T contains not only the states (S_t, I_t, R_t) but also knowledge of who was the infector when an infection occurred and who was removed when a removal occurred, for both of which there is a uniform choice among the I_{t_i} -infected individuals at time t_i .

We now have all the components of equation (1). Inference proceeds using an MCMC approach.

MCMC Moves

For the parameters of the epidemiological process β and γ , we use the Gibbs moves introduced by O'Neill and Roberts (1999). These moves rely on the fact that the distribution $\mathbf{P}(T | \beta, \gamma)$ in equation (5) has for conjugate prior a gamma distribution so that the posterior of these parameters is also a gamma distribution.

For the parameter of the within-host evolutionary process N_{gg} , we use a Metropolis move such that the new value is equal to the old one plus a draw from $\text{Uniform}([-\epsilon, \epsilon])$. This move is accepted with probability equal to the ratio of equation (2) after and before the move, times the ratio of prior probability of N_{gg} after and before the move.

To update the transmission tree T , a single infection event is first chosen at random. If the infection is to the source case, then its date is proposed to be modified by a draw from $\text{Uniform}([-\epsilon, \epsilon])$ (excluding values that would make the transmission to the source case become more recent than the common ancestor of the genealogy G). Otherwise, if the transmission is not to the first case, then it corresponds to a transmission event, that is, a point at which two colors meet on the genealogy. The proposed MCMC update consists of moving this transmission event uniformly at random to another point on the genealogy where it gives a valid coloring, that is, one where 1) there are only $n - 1$ color changes, 2) each leaf is colored in the color c_i of the host it corresponds to, and 3) the color c_i does not exist in the tree after the leaf corresponding to host i . We note that this move may impact the meaning not only of the transmission event being moved but also of other transmission events on the tree so that the

validity of the whole configuration has to be checked. This proposed move is symmetric, and it is accepted with probability equal to the ratio of the products of equations (2) and (5) after and before the move. In the [supplementary information, Supplementary Material](#) online, we discuss the symmetry in more detail and show that the resulting Markov chain is irreducible.

The computational time taken to perform a single iteration of the MCMC scales linearly with the number n of infected individuals, but the number of iterations required to achieve good convergence and mixing properties of the MCMC may vary accordingly. Our implementation of this MCMC algorithm is freely available as a Matlab package at <http://code.google.com/p/transphylo/> (last accessed April 12, 2014).

Application of the Method to a Real-World *M. tuberculosis* Outbreak Data Set

Whole genomes of 33 *M. tuberculosis* were sequenced on an Illumina HiSeq and short reads were aligned against the *M. tuberculosis* CDC1551 reference sequence using Burrows-Wheeler Aligner (BWA; Li and Durbin 2009). SAMtools (Li et al. 2009) mpileup with default parameters identified 20 high-confidence single nucleotide variant (SNV) positions that differed among the isolates, defined as positions called with a quality score of 222, genotype quality of 99, and no indication of strand basis or low depth of coverage. Recognizing that repetitive regions frequently contain erroneous variant calls, we did not include a SNV if it was located within 50 bp of another SNV. Phylogenetic inference was performed with BEAST (Drummond and Rambaut 2007) using the concatenated SNV data labeled with sampling dates. A coalescent model with constant population size (Kingman 1982) was used for the tree prior. More complex priors such as a coalescent with exponential growth prior (Griffiths and Tavaré 1994) or a birth–death epidemiological prior (Stadler et al. 2012) did not make a significant difference to the resulting phylogeny.

Inference under the basic scenario used equation (5) for the prior on the transmission tree with $N = 400$, reflective of the number of individuals in the outbreak community estimated to be at risk of tuberculosis exposure. The second scenario modified equation (5) to incorporate known aspects of the outbreak's epidemiology, including the geographic location of a host, host smear status (positive or negative), and whether the transmission event in a proposed transmission network happened at a time that a host was known to be noninfectious (e.g., at a time before a negative tuberculosis skin test). We modeled infection at a rate $(\beta^+ I^+ + \beta^- I^-)S$ and recovery at a total rate $\gamma(I^+ + I^-)$, for which I^+ and I^- are the numbers of smear-positive and -negative cases. We penalized transmission trees in which cases transmit before they are thought to have become infectious based on their clinical history, trees in which cases receive infection before the time of their most recent negative tuberculosis skin test, and trees in which transmission occurs between cases not known to have been in the same location.

This results in modifications to equation (5), although the principle is the same

$$P(T | \beta, \gamma) = \prod_{i=2}^{2n} \delta_{k_i} \frac{1}{P_{k_i}(t)} \frac{r_{k_i}(t)}{R(t)} R(t) e^{-R(t)(t_i - t_{i-1})} \quad (6)$$

$$= \prod_{i=2}^{2n} \rho_{k_i}(t) e^{-R(t)(t_i - t_{i-1})},$$

where $R(t)$ is the total rate at which events occur, so that $R(t)e^{-R(t)(t_i - t_{i-1})}$ is the probability that time $t_i - t_{i-1}$ elapsed between events; $\frac{r_{k_i}(t)}{R(t)}$ is the probability of the event being type k_i (for example, given that an event occurred after a time interval $t_i - t_{i-1}$, the probability that it was a recovery is $\frac{\gamma(I^+ + I^-)}{\gamma(I^+ + I^-) + (\beta^+ I^+ + \beta^- I^-)S}$), and the population to which the event applies with uniform probability is P_{k_i} . For recoveries $P_{k_i} = I^+ + I^-$ and for infection events, it is either I^+ or I^- corresponding to whether a smear-positive or -negative case was the infector. The penalty δ_{k_i} for the event is either 1 (no penalty), 0.05 if the event contradicts the timing of cases' clinical histories, or 0.005 for a transmission event that occurred when cases were in different locations with no known travel of either case. This reflects a (small) probability that data for cases' locations did not incorporate all travel.

The resulting transmission networks for both scenarios were visualized using Cytoscape v.3.0.2 (Smoot et al. 2011), using a yFiles organic layout and visually encoding the posterior probability of an edge using edge coloring and width. Cytoscape's NetworkAnalyzer module was used to calculate network features, including the clustering coefficient (Barabási and Oltvai 2004) C_n of a given node n in a directed graph:

$$C_n = e_n / (k_n(k_n - 1)), \quad (7)$$

where k_n is the number of neighbors of node n and e_n is the number of links between these k_n neighbors.

Supplementary Material

Supplementary figures S1–S5 are available at *Molecular Biology and Evolution* online (<http://www.mbe.oxfordjournals.org/>).

Acknowledgments

We thank Dr Rob Parker, Dr Sue Pollock, Dr Paul Hasselback, Lori Hiscoe, and Denise McKay for their contributions to the outbreak field investigation, and Dr Patrick Tang, Dr James Johnston, and Dr Mabel Rodrigues for their contributions to the genomics work. C.C. was supported by the Engineering and Physical Sciences Research Council (EPSRC EP/K026003/1 and EP/I031626/1).

References

Alizon S, Luciani F, Regoes RR. 2011. Epidemiological and clinical consequences of within-host evolution. *Trends Microbiol.* 19(1):24–32.

Allen L. 2008. An introduction to stochastic epidemic models. In: Brauer F, van den Driessche P, Wu J, editors. *Mathematical epidemiology* (Lecture notes in mathematics. vol. 1945). Berlin: Springer. p. 81–130.

Barabási A-L, Oltvai ZN. 2004. understanding the cell's functional organization. *Nat Rev Genet.* 5(2):101–113.

Bergstrom CT, McElhany P, Real LA. 1999. Transmission bottlenecks as determinants of virulence in rapidly evolving pathogens. *Proc Natl Acad Sci U S A.* 96(9):5095–6100.

Boeras DI, Hraber PT, Hurlston M, Evans-Strickfaden T, Bhattacharya T, Giorgi EE, Mulenga J, Karita E, Korber BT, Allen S, et al. 2011. Role of donor genital tract HIV-1 diversity in the transmission bottleneck. *Proc Natl Acad Sci U S A.* 108(46):E1156–E1163.

Bouckaert RR. 2010. DensiTree: making sense of sets of phylogenetic trees. *Bioinformatics* 26(10):1372–1373.

Cottam EM, Thébaud G, Wadsworth J, Gloster J, Mansley L, Paton DJ, King DP, Haydon DT. 2008. Integrating genetic and epidemiological data to determine transmission pathways of foot-and-mouth disease virus. *Proc R Soc B Biol Sci.* 275:887–895.

Cottam EM, Wadsworth J, Shaw AE, Rowlands RJ, Goatley L, Maan S, Maan NS, Mertens PPC, Ebert K, Li Y, et al. 2008. Transmission pathways of foot-and-mouth disease virus in the United Kingdom in 2007. *PLoS Pathog.* 4(4):e1000050.

Didelot X. 2013. Genomic analysis to improve the management of outbreaks of bacterial infection. *Expert Rev Anti Infect Ther.* 11(4):335–337.

Didelot X, Bowden R, Wilson DJ, Peto TEA, Crook DW. 2012. Transforming clinical microbiology with bacterial genome sequencing. *Nat Rev Genet.* 13:601–612.

Didelot X, Eyre DW, Cule M, Ip CLC, Ansari MA, Griffiths D, Vaughan A, Connor LO, Golubchik T, Elizabeth M, et al. 2012. Microevolutionary analysis of *Clostridium difficile* genomes to investigate transmission. *Genome Biol.* 13:R118.

Didelot X, Falush D. 2007. Inference of bacterial microevolution using multilocus sequence data. *Genetics* 175(3):1251–1266.

Didelot X, Nell S, Yang I, Woltemate S, van der Merwe S, Suerbaum S. 2013. Genomic evolution and transmission of *Helicobacter pylori* in two South African families. *Proc Natl Acad Sci U S A.* 110(34):13880–13885.

Drummond AJ, Nicholls GK, Rodrigo AG, Solomon W. 2002. Estimating mutation parameters, population history and genealogy simultaneously from temporally spaced sequence data. *Genetics* 161(July):1307–1320.

Drummond AJ, Rambaut A. 2007. BEAST: Bayesian evolutionary analysis by sampling trees. *BMC Evol Biol.* 7:214.

Dye C, Williams BG. 2000. Criteria for the control of drug-resistant tuberculosis. *Proc Natl Acad Sci U S A.* 97(14):8180–8185.

Edwards CTT, Holmes EC, Wilson DJ, Viscidi RP, Abrams EJ, Phillips RE, Drummond AJ. 2006. Population genetic estimation of the loss of genetic diversity during horizontal transmission of HIV-1. *BMC Evol Biol.* 6:28.

Eveillard M, Martin Y, Hidri N, Boussougant Y, Joly-Guillou M-L. 2004. Carriage of methicillin-resistant *Staphylococcus aureus* among hospital employees: prevalence, duration and transmission to households. *Infect Control Hosp Epidemiol.* 25(2):114–120.

Eyre DW, Cule ML, Wilson DJ, Griffiths D, Vaughan A, O'Connor L, Ip CL, Golubchik T, Batty EM, Finney JM, et al. 2013. Diverse sources of *C. difficile* infection identified on whole-genome sequencing. *N Engl J Med.* 369(13):1195–1205.

Ford CB, Lin PL, Chase MR, Shah RR, Iartchouk O, Galagan J, Mohaideen N, Ioerger TR, Sacchettini JC, Lipsitch M, et al. 2011. Use of whole genome sequencing to estimate the mutation rate of *Mycobacterium tuberculosis* during latent infection. *Nat Genet.* 43(5):482–486.

Gardy JL, Johnston JC, Ho Sui SJ, Cook VJ, Shah L, Brodtkin E, Rempel S, Moore R, Zhao Y, Holt R, et al. 2011. Whole-genome sequencing and social-network analysis of a tuberculosis outbreak. *N Engl J Med.* 364(8):730–739.

Gibbons A. 1985. Algorithmic graph theory. Cambridge (United Kingdom): Cambridge University Press.

Gillespie DT. 1976. A general method for numerically simulating the stochastic time evolution of coupled chemical reactions. *J Comput Phys.* 22(4):403–434.

- Golubchik T, Batty EM, Miller RR, Farr H, Young BC, Lerner-Svensson H, Fung R, Godwin H, Knox K, Votintseva A, et al. 2013. Within-host evolution of *Staphylococcus aureus* during asymptomatic carriage. *PLoS One* 8(5):e61319.
- Green PJ. 1995. Reversible jump Markov chain Monte Carlo computation and Bayesian model determination. *Biometrika* 82(4):711–732.
- Grenfell BT, Pybus OG, Gog JR, Wood JLN, Daly JM, Mumford JA, Holmes EC. 2004. Unifying the epidemiological and evolutionary dynamics of pathogens. *Science* 303(5656):327–332.
- Griffiths R, Tavaré S. 1994. Sampling theory for neutral alleles in a varying environment. *Philos Trans R Soc B Biol Sci.* 344:403–410.
- Haaland RE, Hawkins PA, Salazar-Gonzalez J, Johnson A, Tichacek A, Karita E, Manigart O, Mulenga J, Keele BF, Shaw GM, et al. 2009. Inflammatory genital infections mitigate a severe genetic bottleneck in heterosexual transmission of subtype A and C HIV-1. *PLoS Pathog.* 5(1):e1000274.
- Harris SR, Cartwright EJ, Török ME, Holden MT, Brown NM, Ogilvy-Stuart AL, Ellington MJ, Quail MA, Bentley SD, Parkhill J, et al. 2013. Whole-genome sequencing for analysis of an outbreak of methicillin-resistant *Staphylococcus aureus*: a descriptive study. *Lancet Infect Dis.* 13(2):130–136.
- Jombart T, Cori A, Didelot X, Cauchemez S, Fraser C, Ferguson N. 2014. Bayesian reconstruction of disease outbreaks by combining epidemiologic and genomic data. *PLoS Comput Biol.* 10:e1003457.
- Jombart T, Eggo RM, Dodd PJ, Balloux F. 2011. Reconstructing disease outbreaks from genetic data: a graph approach. *Heredity* 106(2):383–390.
- Kass R, Raftery A. 1995. Bayes factors. *J Am Stat Assoc.* 18(7):773–795.
- Keele BF, Giorgi EE, Salazar-Gonzalez JF, Decker JM, Pham KT, Salazar MG, Sun C, Grayson T, Wang S, Li H, et al. 2008. Identification and characterization of transmitted and early founder virus envelopes in primary HIV-1 infection. *Proc Natl Acad Sci U S A.* 105(21):7552–7557.
- Kennemann L, Didelot X, Aebischer T, Kuhn S, Drescher B, Droege M, Reinhardt R, Correa P, Meyer TF, Josenhans C, et al. 2011. *Helicobacter pylori* genome evolution during human infection. *Proc Natl Acad Sci U S A.* 108(12):5033–5038.
- Kingman J. 1982. The coalescent. *Stoch Proc Appl.* 13(3):235–248.
- Köser CU, Ellington MJ, Cartwright EJP, Gillespie SH, Brown NM, Farrington M, Holden MTG, Dougan G, Bentley SD, Parkhill J, et al. 2012. Routine use of microbial whole genome sequencing in diagnostic and public health microbiology. *PLoS Pathog.* 8(8):e1002824.
- Le VTM, Diep BA. 2013. Selected insights from application of whole-genome sequencing for outbreak investigations. *Curr Opin Crit Care.* 19(5):432–439.
- Li H, Durbin R. 2009. Fast and accurate short read alignment with Burrows–Wheeler transform. *Bioinformatics* 25(14):1754–1760.
- Li H, Handsaker B, Wysoker A, Fennell T, Ruan J, Homer N, Marth G, Abecasis G, Durbin R. 2009. The sequence alignment/map (SAM) format and SAMtools. *Bioinformatics* 25(16):2078–2079.
- Lieberman TD, Michel J-B, Aingaran M, Potter-Bynoe G, Roux D, Davis MR, Skurnik D, Leiby N, LiPuma JJ, Goldberg JB, et al. 2011. Parallel bacterial evolution within multiple patients identifies candidate pathogenicity genes. *Nat Genet.* 43(12):1275–1280.
- Marschall J, Mühlemann K. 2006. Duration of methicillin-resistant *Staphylococcus aureus* carriage, according to risk factors for acquisition. *Infect Control Hosp Epidemiol.* 27(11):1206–1212.
- Morelli MJ, Thébaud G, Chadœuf J, King DP, Haydon DT, Soubeyrand S. 2012. A Bayesian inference framework to reconstruct transmission trees using epidemiological and genetic data. *PLoS Comput Biol.* 8(11):e1002768.
- Nylander JAA, Olsson U, Alström P, Sanmartín I. 2008. Accounting for phylogenetic uncertainty in biogeography: a Bayesian approach to dispersal-variance analysis of the thrushes (Aves: Turdus). *Syst Biol.* 57(2):257–268.
- O'Neill PD. 2002. A tutorial introduction to Bayesian inference for stochastic epidemic models using Markov chain Monte Carlo methods. *Math Biosci.* 180:103–114.
- O'Neill PD, Roberts GO. 1999. Bayesian inference for partially observed stochastic epidemics. *J R Stat Soc Ser A.* 162(1):121–129.
- Parker J, Rambaut A, Pybus OG. 2008. Correlating viral phenotypes with phylogeny: accounting for phylogenetic uncertainty. *Infect Genet Evol.* 8(3):239–246.
- Pybus OG, Rambaut A. 2009. Evolutionary analysis of the dynamics of viral infectious disease. *Nat Rev Genet.* 10(8):540–550.
- Robinson K, Fyson N, Cohen T, Fraser C, Colijn C. 2013. How the dynamics and structure of sexual contact networks shape pathogen phylogenies. *PLoS Comput Biol.* 9(6):e1003105.
- Sabat A, Budimir A, Nashev D, Sá-Leão R, van Dijk JM, Laurent F, Grundmann H, Friedrich A. 2013. Overview of molecular typing methods for outbreak detection and epidemiological surveillance. *Euro Surveill.* 18(4):20380.
- Scanvic A, Denic L, Gaillon S, Giry P, Andremont A, Lucet JC. 2001. Duration of colonization by methicillin-resistant *Staphylococcus aureus* after hospital discharge and risk factors for prolonged carriage. *Clin Infect Dis.* 32(10):1393–1398.
- Smoot ME, Ono K, Ruschinski J, Wang P-L, Ideker T. 2011. Cytoscape 2.8: new features for data integration and network visualization. *Bioinformatics* 27(3):431–432.
- Stadler T, Kouyos R, von Wyl V, Yerly S, Böni J, Bürgisser P, Klimkait T, Joos B, Rieder P, Xie D, et al. 2012. Estimating the basic reproductive number from viral sequence data. *Mol Biol Evol.* 29(1):347–357.
- Tavaré S, Balding DJ, Griffiths R, Donnelly P. 1997. Inferring coalescence times from DNA sequence data. *Genetics* 145(2):505.
- Walker TM, Ip CL, Harrell RH, Evans JT, Kapatai G, Dedicoat MJ, Eyre DW, Wilson DJ, Hawkey PM, Crook DW, et al. 2013. Whole-genome sequencing to delineate *Mycobacterium tuberculosis* outbreaks: a retrospective observational study. *Lancet Infect Dis.* 13(2):137–146.
- Walker TM, Lalor MK, Broda A, Ortega LS, Morgan M, Parker L, Churchill S, Bennett K, Golubchik T, Giess AP, et al. 2014. Assessment of *Mycobacterium tuberculosis* transmission in Oxfordshire, UK, 2007–12, with whole pathogen genome sequences: an observational study. *Lancet Respir Med.* 2:285–292.
- Young BC, Golubchik T, Batty EM, Fung R, Lerner-Svensson H, Rimmer AJ, Cule M, Ip CL, Didelot X, Harding RM, et al. 2012. Evolutionary dynamics of *Staphylococcus aureus* during progression from carriage to disease. *Proc Natl Acad Sci U S A.* 109:4550–4555.
- Ypma RJF, Bataille AMA, Stegeman A, Koch G, Wallinga J, van Ballegooijen WM. 2012. Unravelling transmission trees of infectious diseases by combining genetic and epidemiological data. *Proc R Soc B Biol Sci.* 279:444–450.
- Ypma RJF, van Ballegooijen WM, Wallinga J. 2013. Relating phylogenetic trees to transmission trees of infectious disease outbreaks. *Genetics* 195:1055–1062.